

PACS numbers: 07.07.Df; 42.40.Eq; 42.40.My
DOI: 10.1070/QE2010v040n02ABEH014169

Holographic sensors for diagnostics of solution components

A.V. Kraiskii, V.A. Postnikov, T.T. Sultanov, A.V. Khamidulin

Abstract. **The properties of holographic sensors of two types are studied. The sensors are based on a three-dimensional polymer-network matrix of copolymers of acrylamide, acrylic acid (which are sensitive to the medium acidity and bivalent metal ions) and aminophenylboronic acid (sensitive to glucose). It is found that a change in the ionic composition of a solution results in changes in the distance between layers and in the diffraction efficiency of holograms. Variations in the shape of spectral lines, which are attributed to the inhomogeneity of a sensitive layer, and nonmonotonic changes in the emulsion thickness and diffraction efficiency were observed during transient processes. The composition of the components of a hydrogel medium is selected for systems which can be used as a base for glucose sensors with the mean holographic response in the region of physiological glucose concentration in model solutions achieving 40 nm/(mmol L^{-1}). It is shown that the developed holographic sensors can be used for the visual and instrumental determination of the medium acidity, alcohol content, ionic strength, bivalent metal salts and the quality of water, in particular, for drinking.**

Keywords: *holographic sensors, diagnostics of solutions, glucose, heavy metals.*

At present optical sensors for measuring considerable concentrations of specific components of solutions and their parameters attract quite persistent worldwide interest. The advantage of these sensors is that they permit one to determine simply concentrations both instrumentally and visually. These sensors include holographic sensors [1] and photonic-crystal sensors [2]. They can be used for measuring the concentration of protons (solution acidity), heavy metal ions [3, 4], glucose in blood [5, 6] and other biological liquids [7], and bacterium spores [8].

Holographic sensors [1] are quite promising because they are highly sensitive, are easy to operate, provide a high enough accuracy and can be used for various applications. At present they belong to sensors with a moderate sensitivity from tens to thousands of μmol L^{-1}, depending on the type of the analysed component and the design and composition of the sensor matrix. Such a sensitivity range is required, for example, in measurements of the glucose concentration in blood and other biological liquids.

Holographic sensors are based on a polymer hydrogel matrix doped with nanosize solid grains so that their concentration changes periodically in space and the mean distance between the grains is much smaller than the visible-light wavelength. Such a structure illuminated by white light, when the diffraction efficiency of a hologram is not too high (transmission is close to unity) reflects narrow-band emission whose wavelength inside the medium for normally incident light is equal to the doubled period of layers. Special components embedded into the matrix cause a change in the hydrogel swelling under the action of a tested component of solution. This leads to the change in the period of the structure and, therefore, in the reflected radiation wavelength. By measuring this wavelength with the help of a monochromator or observing it visually, we can estimate the concentration of tested components (metal ions, glucose, acidity, etc.).

The main goal of our paper at this stage is the development of sensors for measuring the glucose concentration in blood – low-cost and simple to handle nonconsumable test plates. In addition, we assume the possibility of the development of sensors to control the conditions of transport and storage of vaccines, serums, ferment preparations, food, and also simple test systems in homes. In our opinion, the study of mechanisms of changes in the holographic response will make it possible to perform the precise adjustment of a sensor for particular operating conditions.

We obtained holograms in usual photographic process. By exposing photographic emulsions in a tested solution to radiation from a He – Ne laser in the counterpropagating-beam scheme, we obtained silver nanograins [1, 9 – 12] with the period of layers providing the location of reflected radiation peaks in the operating region of the spectrometer. We investigated a number of matrices of different compositions and designs. Matrices based on copolymers of acrylamide with ionogen comonomers are sensitive to the solution acidity and ionic strength, while matrices based on aminophenylboronic acid are sensitive to glucose. We studied in the paper the main properties of these sensors.

Figure 1 shows the typical reflection spectrum of the sensitive layer of a sensor. The reflection spectrum for the ideal layer should be described by the function $(\sin x/x)^2$. In

A.V. Kraiskii, T.T. Sultanov P.N. Lebedev Physics Institute, Russian Academy of Sciences, Leninsky prosp. 53, 119991 Moscow, Russia; e-mail: kraiski@sci.lebedev.ru
V.A. Postnikov, A.V. Khamidulin Research Institute of Physicochemical Medicine, Federal Agency of Public Health and Social Development, ul. Malaya Pirogovskaya 1a, 119992 Moscow, Russia; e-mail: vladpostnikov@mail.ru

Received 22 June 2009
Kvantovaya Elektronika **40** (2) 178 – 182 (2010)
Translated by M.N. Sapozhnikov

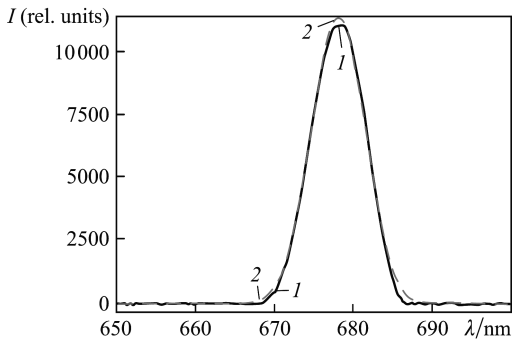

Figure 1. Experimental sensitivity of the reflection spectrum of the sensor (*1*) and its approximation by a Gaussian of width 8 nm (*2*).

our case, the spectrum is well described by a Gaussian. This is explained by the imperfect arrangement of silver grain layers.

Note that metal silver grains are located in the hologram in a very complex environment containing molecules and ions of solution, elements of the hydrogel matrix. When the solution composition is changed, the composition of ions in solution and the structure of the matrix itself are redistributed. As a result, the sensor response, i.e. the mean wavelength of reflected radiation changes, and the radiation intensity also changes due to the change in the diffraction efficiency of the hologram. Figure 2a shows the response of the sensor located in the hydrochloric acid solution titrated with NaOH (the solution acidity was measured with a usual pH-meter). During titration, the reflected radiation wavelength and diffraction efficiency change drastically at the point where the solution acidity drastically changes. In this case, the diffraction efficiency changed almost by an order of magnitude. This means that the change in the ionic composition is accompanied not only by the swelling of hydrogel but also by a strong change in the scattering properties of a holographic layer. This fact was unknown before our studies [9–12]. Figure 2b presents the dependences from Fig. 2a reduced to the same scale by using the following algorithm. For some dependence $F(m)$, we determined the maximum (A) and minimum (B) of its values for the boundary values of its argument m (in Fig. 2, the volume of the added alkali solution): $A = \max(F(0), F(m_{\max}))$, $B = \min(F(0), F(m_{\max}))$. Then, the dependence $F(m)$ was transformed to the dependence $f(m)$ as $f(m) = (F(m) - B)/(A - B)$. One can see from Fig. 2b that all the features of the titration curve are reflected in optical characteristics, i.e. they can be used to control the acidity. Note that the sign of a change in the diffraction efficiency during a change in the amount of added alkali is opposite to the sign in the wavelength change.

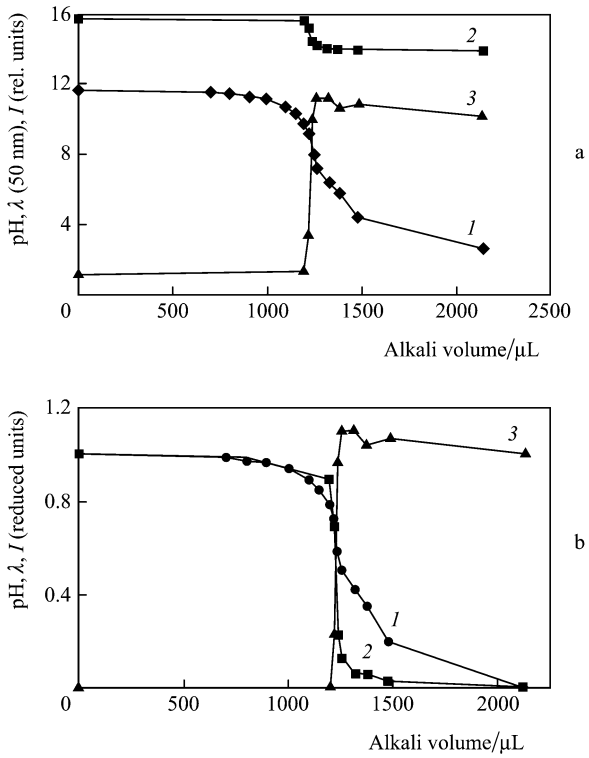

Figure 2. Dependences of the acidity (measured in solution) (*1*), the wavelength (*2*), and intensity (*3*) of radiation reflected from a sensor in the hydrochloric acid solution during its titration with NaOH (a) and also the so-called reduced dependences (see the text) (b).

Figure 3 shows the responses of sensors to metal ions in a broad concentration range from 10^{-7} to 10^{-1} M. They can be divided into three groups. The sensor is most sensitive to Pb^{2+} and Co^{3+} ions (from 10^{-5} M). The sensor sensitivity to Mn^{2+} and Sr^{2+} ions was two orders of magnitude lower. Note that the sensor sensitivity to the alkali metal ions Na^+ and K^+ is an order of magnitude lower than to Pb^{2+}. In this case, unlike other metal ions, first the swelling of hydrogel occurs (wavelength increases) and then its compression (wavelength decreases).

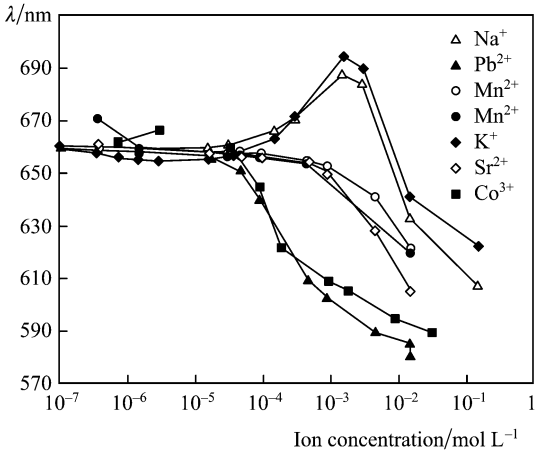

Figure 3. Responses of sensors to different metal ions.

Thus, the sensor can be use for determining the presence of metal ions in water. Figure 4a presents the reflection spectra of the sensor located in the lead salt solution in distilled water ($\lambda = 542$ nm) with concentration 5×10^{-3} M and in mineral water containing calcium salts at concentration 3×10^{-3} M ($\lambda = 585.4$ nm). Sensors can be used repeatedly after regeneration, by washing them, for example, in sodium citrate and then in distilled water. In this case, the sensor response rapidly passes to the IR region ($\lambda = 860$ nm) and then slowly passes to the stationary state (735 nm). Figure 4b shows the typical kinetics of the response maximum in this case. For tap water, the position of the stationary response is closer to its position for mineral water

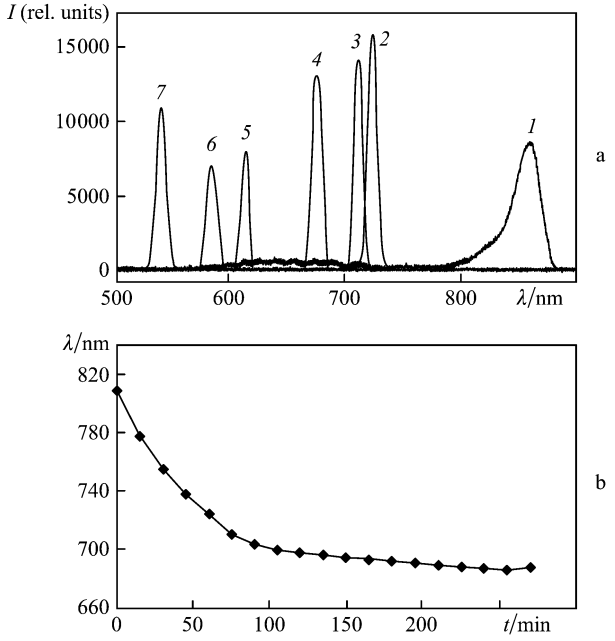

Figure 4. Sensor response to metal ions in water. Reflection spectra in distilled water after the transfer of the sensor from the citrate solution ($\lambda = 860$ nm) (*1*); distilled water (stationary state) ($\lambda = 724$ nm) (*2*); tap water after an Aquaphor filter ($\lambda = 711.7$ nm) (*3*); tap water after Barrier filter ($\lambda = 676.3$ nm) (*4*); cold tap water ($\lambda = 615.2$ nm) (*5*); mineral water containing Ca^{2+} ions at concentration 3×10^{-3} M ($\lambda = 584.4$ nm) (*6*); lead salt solution in distilled water with the concentration of Pb^{3+} ions 5×10^{-3} M ($\lambda = 542$ nm) (*7*) (a) and the shift of the response wavelength of a sensor in distilled water to the stationary state after regeneration (b).

($\lambda = 615.2$ nm), which we explain by the presence of metal salts in tap water. The maxima of the reflection lines in this water after filtration by household filters are located at 676 nm (Barrier filter) and 711.7 nm (Aquaphor filter).

Figure 5 shows the time dependence of the reflection line shape during the transfer of the sensor based on aminophenylboronic acid from the citrate buffer to distilled water and back. This change is reversible. The complex shape of the line is explained by the inhomogeneous distribution of the distance between silver layers over depth. One can see that the diffraction efficiency decreases during layer swelling.

Figure 6a presents the time dependences of the reflection line wavelength for another aminophenylboronic acid sensor

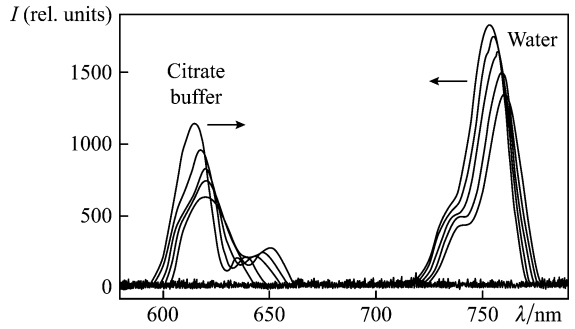

Figure 5. Change in the reflection line shape during the transfer of a senor from the citrate buffer to distilled water (on the right) and back (on the left). The time step is 0.5 s. The arrows indicate the direction of the line shift in time for each group of the lines.

after the replacement of the alkali solution in a cell by the acid solution and vice versa (transition processes). The wavelength was measured during swelling and transition to the stationary state. In this case, the swelling changes monotonically and approximately exponentially. Figure 6b shows the time dependence of the reflection line wavelength in the transition process after the replacement of the citrate buffer by distilled water. The initial state of this sensor was not stationary. The time dependences of the reflection wavelength and intensity are nonmonotonic, their signs being opposite. The nonmonotonic behaviour can be explained by the complicated character of variations in the ionic composition of solution in the emulsion. This effect requires additional studies.

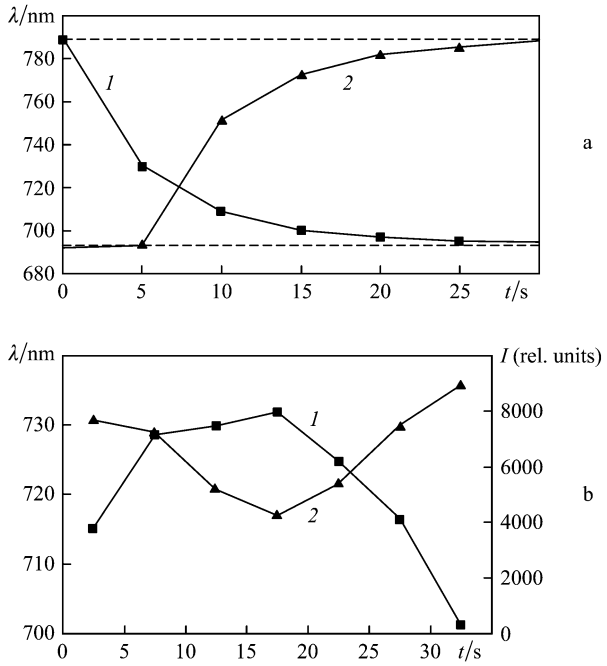

Figure 6. Reflection line wavelengths during the transfer of a sensor based on aminophenylboronic acid from alkali to acid [compression, (*1*)] and [swelling, (*2*)] (a) and the reflection line wavelength (*1*) and intensity (*2*) during the transfer of the sensor from the citrate buffer to distilled water (b).

To adjust a sensor to certain operating conditions, it is necessary to select matrix parameters. This can be performed by varying the matrix design and selecting proper comonomers and their concentrations. Figure 7 shows the dependences of the reflection line wavelength on the solution acidity for matrices of different compositions. One can see that the properties of the sensor response can be controlled in a broad range.

By investigating the properties of sensors in detail, we optimised the responses of various sensors to glucose. Their concentration dependences are shown in Fig. 8a. One can see that the sensor sensitivity changes from 4.3 to 32 nm/(mmol L^{-1}).

Figure 8b presents the concentration dependence of the reflection line wavelength in the physiological concentration range of glucose for a sensor with a mean sensitivity of 18.4 nm/(mmol L^{-1}). One can see that almost all the responses are located in the IR region and this makes the visual control impossible. We can pass to the visible region

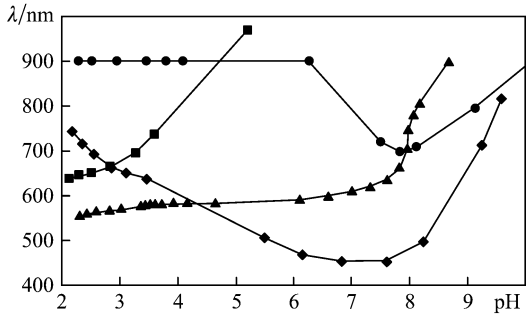

Figure 7. Dependences of the reflection line wavelength on the solution acidity for matrices of different compositions.

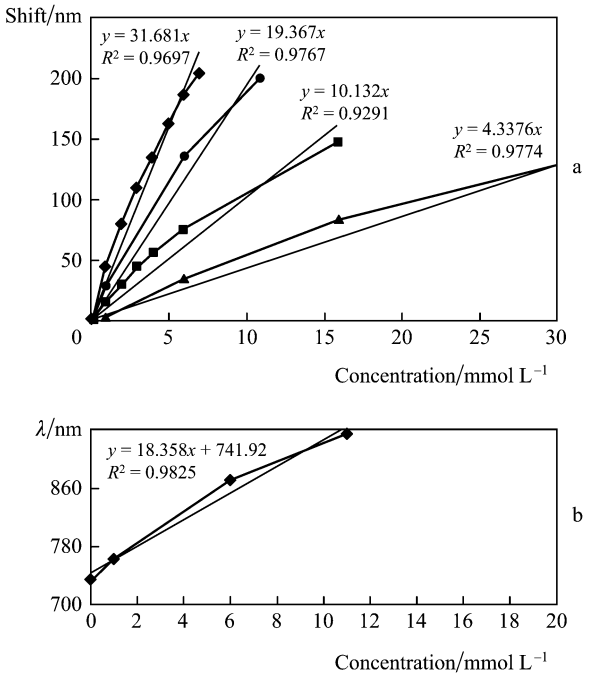

Figure 8. Dependences of the reflection line wavelength on the glucose concentration for different sensors (a) and this dependence in the physiological glucose concentration region for a sensor with a mean sensitivity of 18.4 nm/(mmol L^{-1}) (b). The straight lines are approximations of experimental curves by proportional functions described by presented equations with determination coefficients R^2.

Table 1. Parameters of the sensor response for physiological glucose concentrations.

Glucose concentration/ mmol L^{-1}	Line maximum wavelength [for the sensitivity 18.4 nm/(mmol L^{-1})] /nm	Detuning from the line maximum wavelength for the zero concentration/nm	Line maximum wavelength [for the sensitivity 30 nm/(mmol L^{-1})] /nm
0	733.1	0	450
1	761.5	28.4	478.4
5	869	135.9	585.9
10	933.5	200.4	650.4

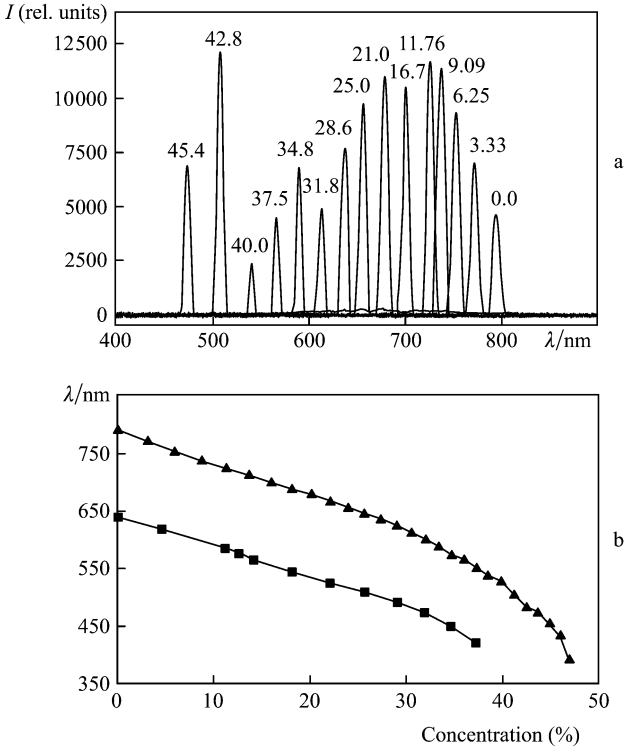

Figure 9. Reflection spectra of sensors based on acrylic acid at different concentrations of ethanol solutions (the ethanol concentration is indicated in %) (a) and the reflection line wavelengths for sensors based on acrylic acid (upper curve) and aminophenylboronic acid (lower curve) (b).

by recording a hologram in the blue light, for example, by radiation from a 446-nm helium–cadmium laser. To preserve the same line shifts on passing to the wavelength ~ 450 nm near the zero concentration, it is necessary to enhance the sensor sensitivity up to 30 nm/(mmol L^{-1}), which corresponds to the latter type of sensors that we obtained. In this case, the reflection line in the concentration region from 0 to 10 mmol L^{-1} will lie between 450 and 650 nm (see Table 1).

Figure 9 shows the responses of sensors for matrices of two types for different concentrations of ethanol in water. Figure 9a presents the reflection lines of a sensor based on acrylic acid for different concentrations of ethanol in water, while Fig. 9b shows the dependences of the reflection line wavelength on the ethanol concentration for this sensor and a sensor based on aminophenylboronic acid. The reflection line wavelength at the zero concentration depends both on the properties of the sensor matrix and on the recording conditions of holograms and can be changed in a controllable way within some range. The concentration dependence in the ethanol solution differs from that upon titration because in this case the decrease in swelling is probably caused by simple dehydration of solution inside the matrix, without ionisation.

Thus, we have developed the method for manufacturing holographic sensors of different types. We have found that the change in the ionic composition of solution is accompanied by the change in the distance between silver nanograin layers and in the diffraction efficiency of holograms. Transition processes revealed variations in the reflection line shape, caused by the inhomogeneity of the sensitive layer, and nonmonotonic changes in the emulsion thickness and diffraction efficiency. We have selected the composition of components of the hydrogel medium for the systems that can be used as bases for glucose sensors. The maximum mean holographic response in the region of physiological concentrations of glucose (1–20 mmol L^{-1}) per 1 mmol L^{-1} of glucose in model solutions achieves 40 nm/(mmol L^{-1}) in these sensors. It has been shown that holographic sensors

can be used to determine the acidity of media, ethanol concentration, ionic strength, bivalent metal salts, and the quality of water, in particular, for drinking.

Acknowledgements. This work was supported by the Program of Fundamental Studies 'Fundamental Sciences for Medicine' of the Presidium of RAS.

References

1. Marshall A.J., Lowe Ch.R., et al. *J. Phys. Condens. Matter*., **18**, 619 (2006); Lowe Ch.R., Millington R.B., Bluth J., Mayes J.E., Patent USA No. 5989923, data publ. 1999-11-23.
2. Alexeev V.L., Das S., Finegold D.N., Asher S.A. *Clinical Chem*., **50** (12), 2353 (2004).
3. Marshall A.J., Young D.S., Kabilan S., Hussain A., Blyth J., Lowe Ch.R. *Anal. Chim. Acta*, **527**, 13 (2004).
4. Madrigal-Gonzalez B.M., Christie G., Davidson C.A.B., Blyth J., Lowe Ch.R. *Anal. Chim. Acta*, **528**, 219 (2005).
5. Kabilan S., Marshall A.J., Sartain F.K., Mei-Ching Lee, Hussain A., Xiaoping Yang, Blyth J., Karangu N., James K., Zeng J., Smith D., Domschke A., Lowe Ch.R. *Biosensors and Bioelectronics*, **20**, 1602 (2005).
6. Horgan A.M., Marshall A.J., Key S.J., Dean K.E.S., Creasy C.D., Kabilan S. *Biosensors and Bioelectronics*, **21**, 1838 (2006).
7. Xiaoping Yang, Xiaohan Pan, Blyth J., Lowe Ch.R. *Biosensors and Bioelectronics*, **23** (6), 899 (2008).
8. Bhatta D., Christie G., Madrigal-Gonzalez B., Blyth J., Lowe C.R. *Biosensors and Bioelectronics*, **23**, 520 (2007).
9. Postnikov V.A., Kraiskii A.V., Sultanov T.T., Tikhonov V.E. *Proc. XVIII International School-Seminar 'Spectroscopy of Molecules and Crystals'* (Beregove, Crimea, Ukraine, 2007) p. 261.
10. Kraiskii A.V., Postnikov V.A. Sultanov T.T., Tikhonov V.E. in *Tez. dokl. konf. 'Fundemetal'nye nauki – meditsine'* (Abstracts of Papers of Conference on Fundamental Sciences for Medicine) (Moscow, 2007) p. 79.
11. Kraiskii A.V., Postnikov V.A., Sultanov T.T., Tikhonov V.E. *Al'man. Klin. Med*., **17** (2), 108 (2008).
12. Kraiskii A.V., Postnikov V.A., Deniskn V.V., Sultanov TT., Tikhonov V.E., Khamidulin A.V. in *Trudy Mezhdunar. konf. 'Preobrazovanie energii sveta pri fotosinteze'* (Proceedings of International Conference on Transformation of Light in Photosynthesis) (Pushchino, 2008) p. 221.